



## Characterization of the nucleus, cutting edge and failure detection in NiTi instruments for endodontic retreatment

Daniel de Almeida Decurcio<sup>a</sup>, Julio Almeida Silva<sup>a</sup>, Mateus Gehrke Barbosa<sup>a</sup>, Lucas Silva Chaves<sup>a</sup>, Marco Antônio Zaiden Loureiro<sup>a</sup>, Carlos Estrela<sup>a</sup>

### ABSTRACT

**OBJECTIVE:** To characterize the nucleus, cutting edge and to detect defects in surfaces of nickel-titanium (NiTi) instruments for endodontic retreatment.

**METHODS:** The selected endodontic instruments (D-RaCe, ProTaper retreatment and Mtwo retreatment) were evaluated prior to their use in 30- and 50-fold magnification in scanning electron microscopy (SEM), for linear measurements of lateral cut edge areas and of the nucleus and the ratio between these measures. After use in simulated canals, faults in the active surface were analyzed by SEM with 30 and 50 times magnification, and 200 times magnification when faults were found. The images were examined by three evaluators, whose measurements were previously calibrated. The defects analyzed were crack, blunt and barb, and data were tabulated for analysis.

**RESULTS:** The instruments studied differed in results. The D-RaCe system instruments had the highest nucleus:edge ratio, while ProTaper retreatment instruments yielded the lowest ratio. All instruments presented some defect, with the instruments Mtwo retreatment presenting two instruments with defects.

**CONCLUSION:** All analyzed instruments presented some type of failure after using them for removal of the filling material of simulated root canals. The D-RaCe system presented the highest edge measurements and the smallest nucleus measurements, contrary to the ProTaper retreatment system, which presented the smallest edge measurements and the largest core measurements.

**Keywords:** electron scanning microscopy; endodontics; retreatment.

<sup>a</sup> Dental School, Federal University of Goiás, Goiânia, Goiás, Brazil

### Caracterização do núcleo, aresta de corte e detecção de falhas em instrumentos de NiTi para retratamento endodôntico

#### RESUMO

**OBJETIVO:** Caracterizar o núcleo, aresta de corte e detectar falhas em superfícies de instrumentos de níquel-titânio (NiTi) para retratamento endodôntico.

**MÉTODOS:** Instrumentos endodônticos (D-RaCe; ProTaper retratamento e Mtwo retratamento) foram mensurados linearmente nas áreas da aresta lateral de corte e do núcleo, além da razão entre estas medidas. Imagens em microscopia eletrônica de varredura (MEV) foram obtidas em aumento de 30 e 50 vezes. Posterior ao uso em canais simulados, estes instrumentos foram novamente analisadas frente as falhas nas superfícies ativas por MEV, em aumentos de 30 e 50 vezes, e 200 vezes. As imagens foram examinadas por três avaliadores, previamente calibrados. Os defeitos analisados incluíram: trinca, embotamento e farpa. Os dados foram tabulados para análise descritiva.

**RESULTADOS:** Os instrumentos estudados apresentaram resultados diferentes entre si. Os instrumentos do sistema D-RaCe apresentaram maior proporção de núcleo/aresta, enquanto os instrumentos ProTaper Retratamento mostraram a menor proporção. Todos os instrumentos apresentaram algum tipo de defeito, sendo que os instrumentos Mtwo Retratamento apresentaram dois instrumentos com defeitos.

**CONCLUSÃO:** Todos os instrumentos apresentaram algum tipo de falha após uso em desobturação de canais radiculares simulados. Os instrumentos do sistema D-RaCe apresentaram as maiores medidas de arestas e as menores medidas de núcleo, ao contrário do sistema ProTaper Retratamento que apresentou as menores medidas de arestas e as maiores medidas de núcleo.

**Palavras-chave:** microscopia eletrônica de varredura; endodontia; retratamento.

#### Correspondence:

Daniel de Almeida Decurcio  
[daniel@endoscience.com.br](mailto:daniel@endoscience.com.br)

Received: January 13, 2018

Accepted: March 26, 2018

**Conflict of Interests:** The authors state that there are no financial and personal conflicts of interest that could have inappropriately influenced their work.

**Copyright:** © 2017 Decurcio et al.; licensee EDIPUCRS.

This work is licensed under a Creative Commons Attribution 4.0 International License.



<http://creativecommons.org/licenses/by/4.0/>

## INTRODUCTION

Endodontic retreatment represents a therapeutic procedure indicated when the failure of the initial endodontic treatment is verified, identified by the presence of developing apical periodontitis. Failures in endodontic therapeutic planning, root canal preparation, root canal filling and tooth restoration should be avoided, since they negatively impact on and result in doubtful prognosis [1].

The nickel-titanium (NiTi) alloys of endodontic instruments have allowed advances in treatment and retreatment [2]. The surface of these instruments manufactured with NiTi alloys may influence the fracture of the endodontic instrument [3,4]. The properties of these alloys and their behaviors within curved root canals have been the subject of discussion since their introduction into endodontics [5-16].

Knowledge of the geometric characteristics and implications in the mechanical behavior of the instruments is essential to the professional. The results of endodontic procedures depend on the characteristics of the instruments used and on the professional's ability [17]. Two fracture characteristics of endodontic instruments have been reported [17], including rotational bending and torsional fracture. The first occurs when the instrument is used in a curved root canal, and it affects the contraction of the instrument in the internal area of its curvature and affects the traction in the external area. This deformation causes alternating tensions of traction and contraction to subject the material to cumulative microstructural changes that promote the appearance and increase of cracks, which leads to fracture when it is submitted to its resistance limit. A large diameter of the instrument at the point of maximum stress concentration reduces the number of cycles to a fatigue fracture [17-19]. Another way of fracture is torsion. This occurs when the tip of the instrument is attached to the wall of the root canal and a rotational force is applied to the instrument, exceeding the limit of resistance to fracture by torsion of the instrument. Among several factors that can influence the resistance are the conicity, the design of the instrument and the diameter of the nucleus. The maximum angle in torsion or rotation is smaller than the large diameter of the instrument [17, 20].

Different studies have evaluated the effectiveness of various rotatory instruments, especially in the removal of the root filling material [21-26]. However, there is a need to characterize the instrument structure and possible failure detection after retreatment. The dimension of the edge can be related to the dimension of the nucleus and can thus directly influence the factors associated with the occurrence of instrument fractures, such as the amount of metal alloy and, consequently, the flexibility of the instrument. The relationship between the cutting edge and the nucleus of the rotary endodontic instruments for retreatment, available on the market, should be better understood. This study characterized

the nucleus, the lateral cutting edge and surface defects of nickel-titanium endodontic instruments for retreatment.

## MATERIAL AND METHODS

Preparation of the sample for analysis in scanning electron microscopy

Instruments with a D0 diameter of 0.25 mm and a length of 25 mm were used. Three instruments from each NiTi system for root canal retreatment were studied: D-RaCe® (FKG Dentaire, La Chaux de Fonds, Switzl); ProTaper retreatment® (Dentsply Maillefer, Ballaigues, Switzerland); Mtwo retreatment® (VDW, Munich, Germany).

The samples were analyzed in the Laboratory of Scanning Electron Microscopy of the Faculty of Physics of Federal University of Goiás (LabMic), after being fixed in stubs of the instruments, primarily for analysis of side A (characterized by the convex face of the securing rod in the contra-angle) and later side B (characterized by the flat face of the securing rod in the contra-angle) [27]. Images were obtained in scanning electron microscopy (SEM Leo Stereoscan 420i, Leica Electron Optics, Cambridge Instruments, Cambridge, United Kingdom) with a magnification of 50 times.

### Measurements

The images obtained by the SEM were transferred to the AxioVision (Carl Zeiss Microscopy GmbH, Jena, Germany) software to perform the measurements of the nucleus and lateral cut edge of each instrument in its apical portion.

- Linear measurement of the nucleus – measurement expressed in micrometers ( $\mu\text{m}$ ) of the distance between the lines delimiting the nucleus, at the same point where the upper and lower cut side edge was measured linearly.
- Nucleus area – measure expressed in square micrometers ( $\mu\text{m}^2$ ) of the space between the same meeting points for a measurement of the upper and lower cut side edge (**Figure 1**).
- Linear measurement of the cutting edge – measure expressed in micrometers ( $\mu\text{m}$ ) from the distance between the line delimiting the core and the outermost point of the lateral cutting edge. The region of the edge considered for analysis is represented by the point of meeting between the lateral edge of cut to be measured and the helical canal.
- Cut side edge area – measurement expressed in square micrometers ( $\mu\text{m}^2$ ) of the space between the line delimiting the nucleus and a line that delimits the outermost surface of the edge (**Figure 2**).

After the linear and area measurements, the ratio between the edge measurement and the core measurement of each instrument was calculated.

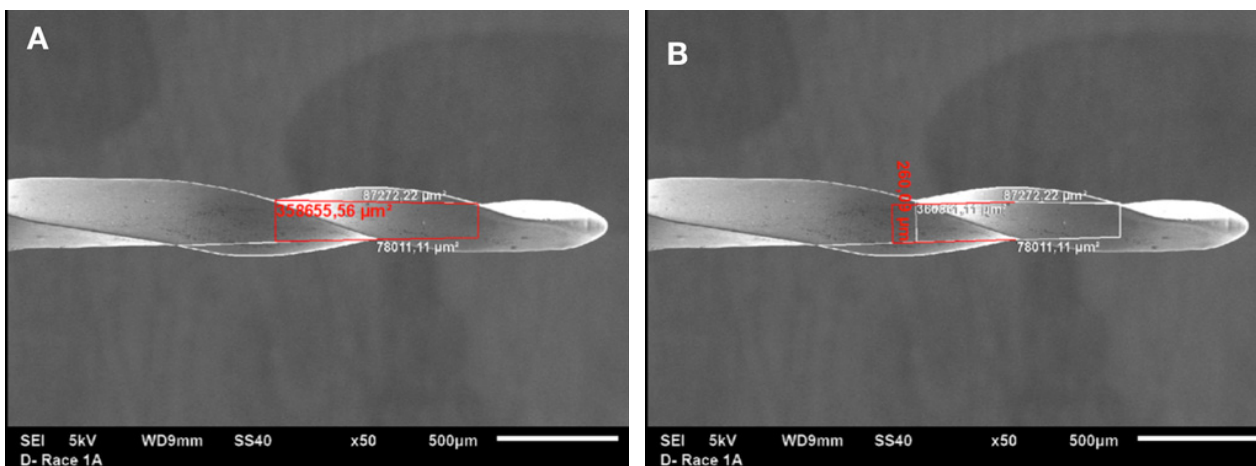


**Figure 1.** Measurement of the nucleus area: space between the same meeting points used for the measurement of the upper and lower cut lateral edge (**image A**); linear measurement: distance between the lateral lines delimiting the nucleus, at the same point where the upper and lower cut lateral edge was measured linearly (**image B**).

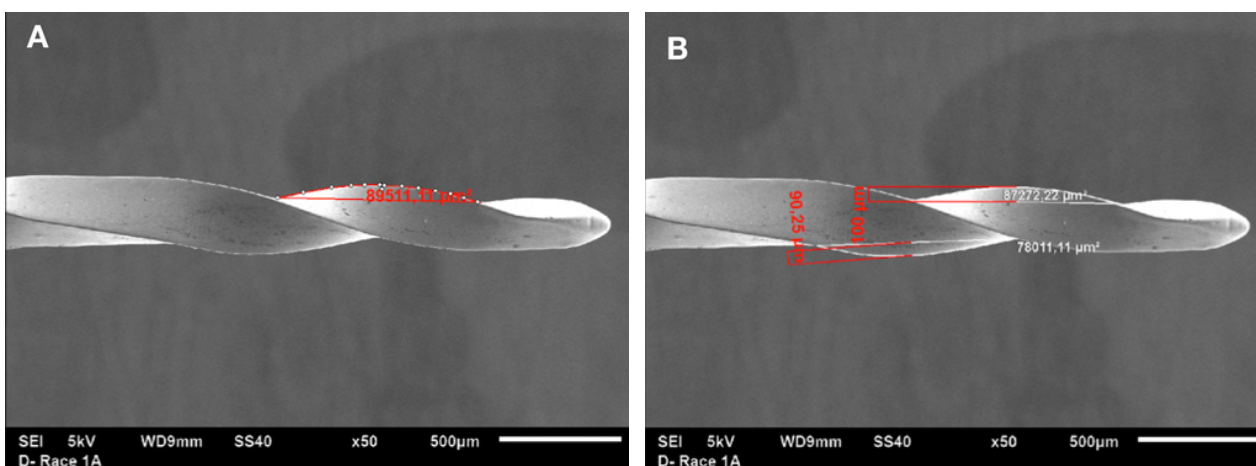


**Figure 2.** Measurement of the cutting edge area: space between the line delimiting the nucleus and a tracing that delimits the outermost surface of the edge (**image A**); linear measurement of the cutting edge: distance between the line delimiting the core and the outermost point of the lateral cutting edge (**image B**).

## Analysis for failure detection

Subsequent to taking measurements, pre-preparation of the simulated acrylic canals was performed. These simulated canals were prepared with rotating NiTi instruments (BioRace® - FKG Dentaire, La Chaux de Fonds, Switzerland) following the manufacturer's indications with conventional irrigation. The canals were filled with AH Plus® cement (Dentsply, Ballaigues, Switzerland) by lateral condensation technique. The same preparation and obturation protocol was followed for all simulated acrylic canals.

Each instrument of each analyzed group was used to unseal and prepare three simulated canals, following the guidelines of each manufacturer. After the instrumentation, the endodontic instruments were analyzed for the presence of active surface defects in the SEM image (Jeol, JSM – 6610, equipped with EDS, Thermo Scientific NSS Spectral Imaging) with secondary electron detector, voltage of

10Kv, working distance (WD) of 10 mm, and diameter of the beam 40 (LabMic). To determine instrument surface defects, the active part was divided into eight parts of 2 mm each (D0–D16) nominated as a-h: a (D0–D2); b (D2–D4); c (D4–D6); d (D6–D8); e (D8–D10); f (D10–D12); g (D12–D14); h (D14–D16).

A total of 144 SEM images were acquired in 50X magnification for the identification of failures in endodontic instruments. In cases of doubt, magnifications of 200X were obtained for better visualization and detailing of failures. For each instrument (n=9), considering both sides A and B (eight parts, two sides) 16 images were obtained.

Among the criteria for analysis of the instrument surfaces, the following was taken into account: absence (A) – absence of failures; crack (C) – open surface or internal discontinuity, originating from localized stresses, whose values exceed the material breaking limit; barb (B) – sharpening tip forming acute angle, sharp piercing protrusion of cutting

part; blunting (BB) – loss of cutting part (folding of a blade) [27].

The images were examined by three endodontists calibrated in 10% of the samples among the established criteria for the failures of the endodontic instruments, which identified the following defects: "C", "B" and "BB" in each analyzed image (Figure 3). In cases of more than one defect for each image, these were named as previously described. The data analysis was descriptive regarding the average of the areas, the linear measurements and the detection of failures in the endodontic instruments.

## RESULTS

The characterization of the nucleus and cutting edge (mean of the areas and linear measurements on the A and B sides and the edge/nucleus ratio) of the analyzed instruments are described in Table 1. The D-RaCe instruments presented the largest edge measurements and the smallest nucleus, followed by the Mtwo and ProTaper instruments, respectively. SEM analyses revealed C, B and BB defects as observed in Figure 3. All groups presented some type of defect, and the distribution of defects per group is expressed in Table 2.

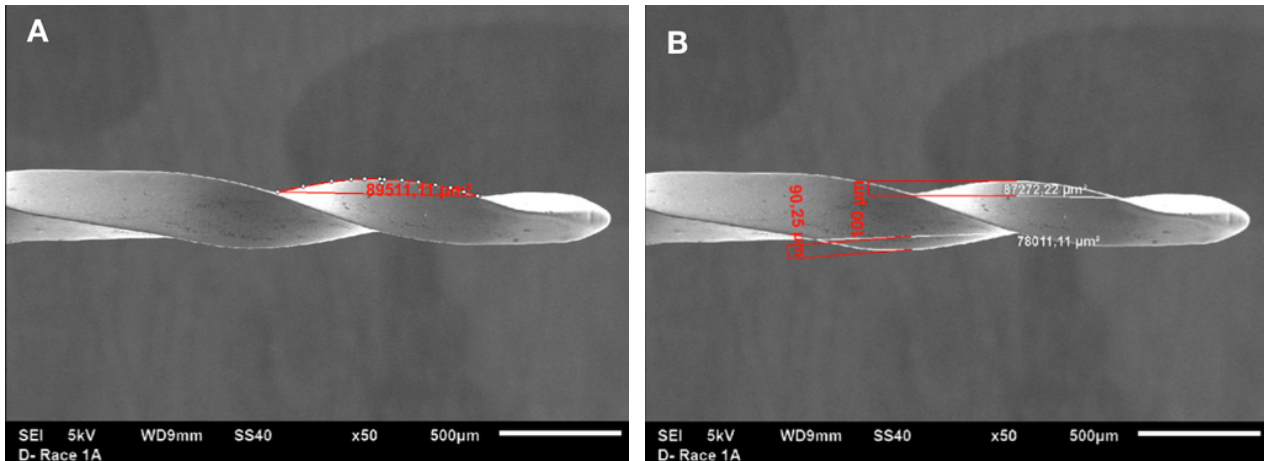


Figure 3. Defects found on instruments after use: crack (C), barb (B) and blunt (BB).

Table 1. Means of the areas and linear measurements on sides A and B, in the regions referring to the edge and the nucleus of the most apical portion of the instruments tested.

Instrument	Nucleus		Edge 1		Edge 1/Nucleus Ratio	
	Area (µm²)	Linear measure	Area (µm²)	Linear measure	Area (µm²)	Linear measure
D-Race 1	355094.445	250.02	88702.77	93.46	0.24980	0.37381
D-Race 2	327202.78	263.47	75644.44	86.66	0.23118	0.32891
D-Race 3	369586.11	263.50	73491.66	83.46	0.19884	0.31673
<b>MEAN</b>	<b>350627.77</b>	<b>259.0016</b>	<b>79279.62</b>	<b>87.86</b>	<b>0.22610</b>	<b>0.33922</b>
ProTaper R 1	395930.56	335.81	53583.33	71.74	0.13533	0.21363
ProTaper R 2	461922.22	391.87	46780.55	66.71	0.10127	0.17023
ProTaper R 3	403513.79	369.13	43844.44	61.85	0.10865	0.16755
<b>MEAN</b>	<b>420455.52</b>	<b>365.60</b>	<b>48069.44</b>	<b>66.76</b>	<b>0.11432</b>	<b>0.18260</b>
Mtwo R 1	353611.11	290	62408.33	61.675	0.17648	0.21267
Mtwo R 2	397791.66	320	64252.78	70.155	0.16152	0.21923
Mtwo R 3	360411.11	303.77	57375	75.035	0.15919	0.47012
<b>MEAN</b>	<b>370604.62</b>	<b>304.5916</b>	<b>61345.37</b>	<b>68.955</b>	<b>0.16552</b>	<b>0.226385</b>

Table 2. Crack, barb and blunt defects found in the different instruments after use.

	D-RaCe			ProTaper			Mtwo		
Crack	-	-	+	-	-	-	-	-	-
Barb	-	-	-	+	-	-	+	-	-
Blunt	-	-	-	-	-	-	+	-	+

+ presence of defect; - absence of defect.



## DISCUSSION

In the endodontic retreatment instruments tested, no visible manufacturing defects were observed in SEM images. After the preparation of the simulated canals, it was identified that all the instruments presented some type of defect after use. The edge:nucleus ratio was 0.33922 for the D-RaCe instruments, whereas the Mtwo retreatment instruments had a ratio of 0.22638 and the ProTaper retreatment ratio was 0.18260. After the measurements, each specimen was used three times, in a total of 27 simulated canals. After analysis of the failures in the SEM images, the three types of flaws were observed. Cracks (C) occurred in an instrument of group 1 (D-RaCe). The barb defects (B) occurred in one specimen of group 2 (ProTaper retreatment) and one of group 3 (Mtwo retreatment). The blunt type (BB) failure occurred in two instruments, both of group 3 (Mtwo retreatment), and in one of them there was also the presence of barb (B). Measurements of the instrument structures were performed from the SEM images, and the AxioVision software was used to obtain linear and area measurements according to previous studies [16,26].

The results found in the present study suggest that the D-RaCe instruments presented greater flexibility and resistance to cyclic fatigue due to its greater edge and smaller nucleus [28,29]. The larger nucleus area in the ProTaper retreatment instrument resulted in less flexibility, but it exhibited greater resistance to fracture by torsion. These results may influence the selection of endodontic instrument to be used.

The mechanical behavior of the instrument can be influenced by its morphometric structural characteristics, such as the conicity, the design of the instrument and the diameter of the nucleus. The diameter of the instrument influences its resistance to fracture, since the larger the diameter of the instrument at the maximum point of stress concentration, the fewer the number of cycles until fatigue fracture [17-19]. In addition, the maximum angle in torsion or rotation of the instrument is smaller for instruments with larger diameter. The ProTaper retreatment instrument had the largest nucleus diameter measured [17, 19].

Other studies [30-32] analyzed the presence of defects after use of nickel-titanium instruments and observed faults involving spiral deformation, deterioration of the angle of cut, cracks and fractures, which increased with prolonged use. The microcracks that were observed as a consequence of these superficial defects propagate and form cracks, and subsequently the metal rupture [3,28]. In the present study, all instruments presented some type of failure that can contribute to the rupture of the endodontic instrument.

The use of simulated acrylic canals allowed a controlled environment and standardization of the canals regarding the caliber, curvature and resistance of the material to be excised, but it is a limitation of this study. Future studies using human teeth, in the presence of root filling material and with a larger sample size, should be performed to better

understand which instruments are reliable for use in root canal retreatment.

## CONCLUSION

All instruments analyzed had some type of failure after use in simulated root canal retreatment procedures. The D-RaCe system showed the greatest edge measurements and the smaller nucleus measures, contrary to the ProTaper retreatment system, which showed lower edge measurements and larger nucleus measurements.

## REFERENCES

- Estrela C, Pécora JD, Estrela CRA. et al. Common operative procedural errors and clinical factors associated with root canal treatment. *Braz Dent J* 2017;28(2):179-90. <https://doi.org/10.1590/0103-6440201702451>
- Esposito PT, Cunningham CJ. A comparison of canal preparation with nickel titanium and stainless steel instruments. *J Endod* 1995;21(4):173-6. [https://doi.org/10.1016/S0099-2399\(06\)80560-1](https://doi.org/10.1016/S0099-2399(06)80560-1)
- Kuhn G, Tavernier B, Jordan L. Influence of structure on nickel-titanium endodontic instruments failure. *J Endod* 2001;27(8):516-20. <https://doi.org/10.1097/00004770-200108000-00005>
- Lopes HP, Elias CN, Estrela C. et al. Assessment of the apical transportation of root canals using the method of the curvature radius. *Braz Dent J* 1998;9(1):39-45.
- Walia H, Brantley WA, Gerstein H. An initial investigation of the bending and torsional properties of nitinol root canal files. *J Endod* 1988;14:346-51. [https://doi.org/10.1016/S0099-2399\(88\)80196-1](https://doi.org/10.1016/S0099-2399(88)80196-1)
- Schäffer E. Root canal instruments for manual use: a review. *Endod Dent Traumatol* 1997;13:51-64. <https://doi.org/10.1111/j.1600-9657.1997.tb00011.x>
- Bürklein S, Schäfer E. Apically extruded debris with reciprocating single-file and full-sequence rotary instrumentation systems. *J Endod* 2012b;38:850-2. <https://doi.org/10.1016/j.joen.2012.02.017>
- Yoo YS, Cho YB. A comparison of the shaping ability of reciprocating NiTi instruments in simulated curved canals. *Rest Dent Endod* 2012;37(4):220-7. <https://doi.org/10.5395/rde.2012.37.4.220>
- Bürklein S, Bente S, Schäfer E. Shaping ability of different single-file systems in severely curved root canals of extracted teeth. *Int Endod J* 2013;46(6):590-7. <https://doi.org/10.1111/iej.12037>
- Lim YJ, Park SJ, Kim HC, Min KS. Comparison of the centering ability of Wave-One and Reciproc nickel-titanium instruments in simulated curved canals. *Rest Dent Endod* 2013;38(1):21-5. <https://doi.org/10.5395/rde.2013.38.1.21>
- Bürklein S, Poschmann T, Schäfer E. Shaping ability of different nickel-titanium systems in simulated S-shaped canals with and without glide path. *J Endod* 2014;40(8):1231-4. <https://doi.org/10.1016/j.joen.2014.01.043>
- Capar ID, Ertas H, Ok E, Arslan H, Ertas ET. Comparative study of different novel nickel-titanium rotary systems for root canal preparation in severely curved root canals. *J Endod* 2014;40(6):852-6. <https://doi.org/10.1016/j.joen.2013.10.010>
- Gergi R, Arbab-Chirani R, Osta N, Naaman A. Micro-computed tomographic evaluation of canal transportation instrumented by different kinematics rotary nickel titanium instruments. *J Endod* 2014;40(8):1223-7. <https://doi.org/10.1016/j.joen.2014.01.039>
- Hwang YH, Bae KS, Baek SH, Kum KY, Lee W, Shon WJ, Chang SW. Shaping ability of the conventional nickel-titanium and reciprocating nickel-titanium file systems: a comparative study using micro-computed tomography. *J Endod* 2014;40(8):1186-9. <https://doi.org/10.1016/j.joen.2013.12.032>
- Nazari Moghadam K, Shahab S, Rostami G. Canal transportation and centering ability of twisted file and reciproc: a cone-beam computed tomography assessment. *Iran Endod J* 2014;9(3):174-9.
- Sampaio FC, Alencar AH, Guedes OA. et al. Chemical elements characterization of root canal sealers using scanning electron microscopy and energy dispersive X-ray analysis. *OHDM – Oral Health Dent Manag* 2014;13:27-34.
- Lopes HP, Siqueira-Jr JF. *Endodontia: biologia e técnica*. Rio de Janeiro: Guanabara Koogan, 2010.
- Lopes HP, Elias CN, Vieira VT, Moreira EJ, Marques RV, de Oliveira JC, Debelian G, Siqueira JF, Jr. Effects of electropolishing surface treatment on the cyclic fatigue resistance of BioRace nickel titanium rotary instruments. *J Endod* 2010;36(10):1653-7. <https://doi.org/10.1016/j.joen.2010.06.026>



19. Lopes HP, Chiesa WM, Correia NR. et al. Influence of curvature location along an artificial canal on cyclic fatigue of a rotary nickel-titanium endodontic instrument. *Oral Surg Oral Med Oral Pathol Oral Radiol Endod* 2011;111(6):792-6. <https://doi.org/10.1016/j.tripleo.2010.12.006>
20. McGuigan MB, Louca C, Duncan HF. Endodontic instrument fracture: causes and prevention. *Br Dent J* 2013;214(7):341-8. <https://doi.org/10.1038/sj.bdj.2013.324>
21. Marques da Silva B, Baratto-Filho F, Leonardi DP. et al. Effectiveness of ProTaper, D-RaCe, and Mtwo retreatment files with and without supplementary instruments in the removal of root canal filling material. *Int Endod J* 2012;45:927-32. <https://doi.org/10.1111/j.1365-2591.2012.02051.x>
22. Zuolo AS, Mello JE Jr, Cunha RS. et al. Efficacy of reciprocating and rotary techniques for removing filling material during root canal retreatment. *Int Endod J* 2013;46:947-53. <https://doi.org/10.1111/iej.12085>
23. Tasdemir T, Er K, Yildirim T, Celik D. Efficacy of three rotary NiTi in removing gutta-percha from root canals. *Int Endod J* 2008;41:191-6. <https://doi.org/10.1111/j.1365-2591.2007.01335.x>
24. Mollo A, Botti G, Principi Goldoni N. et al. Efficacy of two Ni-Ti systems and hand files for removing guttapercha from root canals. *Int Endod J* 2012;45:1-6. <https://doi.org/10.1111/j.1365-2591.2011.01932.x>
25. Rödiger T, Hausdörfer T, Konietzschke F. et al. Efficacy of D-RaCe and ProTaper Universal Retreatment NiTi instruments and hand files in removing gutta-percha from curved root canals – a microcomputed tomography study. *Int Endod J* 2012;45:580-9. <https://doi.org/10.1111/j.1365-2591.2012.02014.x>
26. Zuolo ML, Walton RE. Instrument deterioration with usage: nickel–titanium versus stainless steel. *Quintessence Int* 1997;28:397-402.
27. Silva LRM. Detecção de falhas na superfície ativa de instrumentos de níquel-titânio. Goiânia. Dissertação [Mestrado em Clínica Odontológica] – Universidade Federal de Goiás; 2015.
28. Biz MT, Figueiredo JA. Morphometric analysis of shank-to-flute ratio in rotary nickel–titanium files. *Int Endod J* 2004;37(6):353-8. <https://doi.org/10.1111/j.1365-2591.2004.00755.x>
29. Schafer E, Tepel J. Relationship between design features of endodontic instruments and their properties. Part 3. Resistance to bending and fracture. *J Endod* 2001;27(4):299-303. <https://doi.org/10.1097/00004770-200104000-00018>
30. Thompson SA, Dummer PMH. Shaping ability of Quantec Series 2000 rotary nickel–titanium instruments in simulated root canals: Part 1. *Int Endod J* 1998;31:259–67. <https://doi.org/10.1046/j.1365-2591.1998.00151.x>
31. Svec TA, Powers JM. The deterioration of rotary nickel-titanium files under controlled conditions. *J Endod* 2002;28(2):105-7. <https://doi.org/10.1097/00004770-200202000-00014>
32. Thompson SA. An overview of nickel-titanium alloys used in dentistry. *Int Endod J* 2000;33(4):297-31. <https://doi.org/10.1046/j.1365-2591.2000.00339.x>

